2000

Interaction of binary tropical cyclones in a coupled tropical cyclone-ocean model

Alexander Khain

Isaac Ginis
University of Rhode Island, iginis@uri.edu

Aleksandr Falkovich

Mitia Frumin

Citation/Publisher Attribution

Khain, A., I. Ginis, A. Falkovich, and M. Frumin (2000), Interaction of binary tropical cyclones in a coupled tropical cyclone-ocean model, *J. Geophys. Res.*, *105*(D17), 22337–22354. doi: 10.1029/2000JD900268. Available at: https://doi.org/10.1029/2000JD900268

JOURNAL OF GEOPHYSICAL RESEARCH, VOL. 105, NO. D17, PAGES 22,337-22,354, SEPTEMBER 16, 2000

Interaction of binary tropical cyclones in a coupled tropical cyclone-ocean model

Alexander Khain,[1] Isaac Ginis,[2] Aleksandr Falkovich,[3] and Mitia Frumin[1]

Abstract. The motion and evolution of binary tropical cyclones was investigated using a coupled tropical cyclone-ocean movable nested grid model. The model consists of eight-layer atmospheric and seven-layer ocean primitive equation models. Several regimes of binary storm interaction have been identified, depending on the initial separation distance (d) and differences in storm strengths. At d less than a few hundred kilometers, interacting storms experienced complete merger (CM) or partial merger (PM). At larger d (between about 600 km and 1000 km), three regimes of storm interaction have been found: PM, straining out (SO), characterized by complete disintegration of the weaker storm, and mutual straining out (MSO), characterized by weakening and dissipation of both storms. SO occurred when the interacting storms had substantially different intensities and strengths. MSO was observed when the interacting storms were comparable in size and intensity. In the latter case the storms were unable to approach each other at distances smaller than a certain minimum distance (of about 450-500 km) without being mutually stretched out. Moreover, initial attraction of the storms in this regime was replaced by repulsion, as frequently observed in the western Pacific. At d exceeding about 1000 km, elastic interaction (EI) was found, when the storms interact without any significant changes in their intensity and structure. In additional experiments with a conditional instability of the second kind (CISK) type parameterization of convective heating the storm interaction was very different: The storms were nearly axisymmetric and very compact, and they continued approaching each other until they merged. Thus more realistic simulations of binary storm interaction can be achieved by using a physically more reasonable convective parameterization.

1. Introduction

Two or more tropical cyclones existing simultaneously interact with each other when the separation distance becomes less than about 1450 km [*Brand*, 1970]. These situations occur more frequently in the western and eastern North Pacific [*Ramage*, 1972; *Lander and Holland*, 1993]. Several hurricanes sometimes develop simultaneously over the Atlantic Ocean, too, as was observed, for example, in August 1995. The interaction of tropical cyclones frequently causes sharp changes of their tracks and translation speed. Large forecast errors can be associated with an incorrect assessment of these situations [*Brand*, 1970; *Neumann*, 1981]. The binary vortices can merge or move away depending on the storm structures and intensities and the separation distance. *Dong and Neumann* [1983] found that the distances between storms, initially separated by less than 900 km, decreases with time in 60% of cases. During the mutual approach, one member of the interacting pair usually decays and loses its identity at relatively large distances (of the order of several hundred kilometers) from the surviving (winner) vortex. In other cases, however, attraction of binary storms may sharply change to repulsion after a certain separation distance is reached [*Lander and Holland*, 1993]. Thus different scenarios are possible which determine the final result of interaction between binary tropical storms.

Most previous theoretical and numerical studies of interaction of binary storms were performed using nondivergent barotropic models. *DeMaria and Chan* [1984] suggested that attraction or repulsion of the vortices in a vortex pair is determined by secondary vortices induced by the advection of vorticity of one storm by the tangential circulation of the other. According to the mechanism suggested, there should exist a critical separation distance, so that the storms initially separated by a smaller (larger) distance will attract (repel). According to *DeMaria and Chan* [1984], attraction or repulsion is determined by the sign of the vorticity gradient of one storm in the point of the location of the other storm. *Falkovich et al.* [1995a] (hereafter FKG) argued that attraction or repulsion in the barotropic case is rather determined by the sign of the relative vorticity between interacting storms. The results of numerical studies by *Pokhil et al.* [1990], *Pokhil* [1991], and *Chan and Law* [1995] are consistent with the latter conclusion.

Interaction of three-dimensional (3-D) tropical cyclones is considerably more complex and greatly influenced by baroclinic effects not accounted for barotropic models. *Chang* [1983, 1984], using a 3-D baroclinic model with a prescribed heating function, found that the attraction between binary storms occurred at greater separations than in a corresponding barotropic model. The divergent component of the wind in the 3-D model was suggested to be mainly responsible for the mutual attraction of the storms. *Wang and Holland* [1995] reached a similar conclusion in their 3-D simulations of binary storms. *Wang and Holland* [1995] found that during mutual attraction the stronger storm in a pair always dominates, even when the differences in the storm strengths are very small. The storm resulting from the merger is more intense either of the initial storms. Note that in both studies a

[1] Institute of Earth Sciences, Hebrew University of Jerusalem, Israel.
[2] Graduate School of Oceanography, University of Rhode Island, Narragansett.
[3] Environmental Modeling Center, National Center for Environmental Prediction, Washington, D.C.

Paper number 2000JD900268.
0148-0227/00/2000JD900268$09.00

conditional instability of the second kind (CISK) type parameterization of cumulus convection was used, in which the heating function was set proportional to the vorticity at the lowest model level.

FKG studied the interaction of two tropical cyclones using a coupled atmosphere-ocean model with explicit description of diabatic heating on resolvable scales. In their study, two initially weak vortices were separated by a few hundred kilometers, and the storms began interacting during their development into tropical cyclones. It was found that in contrast to barotropic vortices, positive vorticity between binary storms is a favorable but not sufficient condition for attraction. They also found that evolution and trajectories of binary storms are significantly affected by the interaction of the storms with the ocean.

FKG studied binary storms that were initially separated at fairly small distances. In the present paper we continue to study the interaction of binary storms at considerably larger separation distances and utilizing an improved version of the coupled tropical cyclone-ocean model. Special attention is paid to various regimes of binary storm interactions and how convective parameterization and ocean coupling affect them. The rest of the paper is organized as follows. The coupled tropical cyclone-ocean model is described in section 2. Model initialization and experimental design are presented in section 3. In section 4 we discuss the regimes of binary storm interactions. The role of convective parameterization and the tropical cyclone-ocean coupling on binary storm interaction is investigated in section 5, followed by the summary.

2. The Coupled Tropical Cyclone-Ocean Model

2.1. The Tropical Cyclone Model

The model is based on the primitive equation system in sigma coordinates on the beta plane. The vertical atmospheric structure is represented by eight sigma levels in the troposphere and an isentropic layer above. The tropical cyclone model is described by FKG in detail. Here we present only a brief summary of the most important and new features.

Condensation heating is calculated at resolvable grid scales [*Rosenthal*, 1978, *Khain*, 1979, 1984, FKG], so that cumulus convection is hydrostatic but explicit. To investigate the influence of convective parameterization on storm interactions, the CISK-type parameterization of *Wang and Holland* [1995] is utilized in some numerical experiments. Horizontal turbulent fluxes are described using a nonlinear viscosity scheme similar to that of *Kurihara et al.* [1974]. The vertical turbulent coefficient is assumed to be proportional to the vertical wind shear and calculated as in the work by *Khain* [1979]. All variables at the anemometer level and the fluxes of sensible and latent heat and momentum are calculated using the *Deardorff* [1972] parameterization. The model has five meshes of differing resolutions. The outermost mesh (7680 x 7680 km) is motionless. The other four meshes represent two pairs of telescopically nested movable inner meshes (3200 x 3200 km and 1600 x 1600 km) that follow the centers of corresponding tropical storms. The inner meshes can overlap during the storm interaction. Space increments of the outermost, middle, and finest meshes are 160 km, 80 km, and 40 km, respectively.

Model integration is performed using different time increments for each computational domain: 6 min, 3 min, and 1.5 min, corresponding to the outermost, middle, and innermost domains. The rules defining the sequence of time integration are similar to those used by *Kurihara and Tripoli* [1979]. At each time step, a version of the Lax – Wendroff scheme is applied. In this scheme, the staggering is used for both the horizontal and vertical directions.

2.2. The Ocean Model

The ocean model is a multilayer, primitive equation ocean model which was used by *Bender et al.* [1993] for studying the upper ocean response to a moving tropical storm in both uncoupled and coupled air-sea configurations. A detailed description of the ocean model and comparisons of the model simulations with observations are given by *Bender et al.* [1993]. We highlight here only the main features utilized in this study.

The vertical ocean structure is represented by a surface mixed layer and a specified number of layers below (seven for the current set of experiments). The mixed layer is considered as a turbulent boundary layer that exchanges momentum and heat with the atmosphere at its surface and with the thermocline by entrainment at its base. The turbulent momentum and the heat fluxes at the free surface are equal to the surface wind stress and total (latent and sensible) heat flux provided by the tropical cyclone model. The vertical turbulent mixing at the mixed layer base is computed from the scheme formulated by *Deardorff* [1983]. The ocean model performance was tested by *Ginis et al.* [1993] using the field observations of the ocean response to Hurricane Norbert (1984) and demonstrated a good skill in simulating the sea surface temperature response. The computational domain contains 213 x 213 grid points, with a spatial increment of 40 km, similar to the finest resolution of the tropical cyclone model. The finite difference equations are formulated on the staggered Arakawa - B grid. The time integration proceeds with a version of the splitting method described by *Ginis and Sutyrin* [1995].

3. Model Initialization and Experimental Design

In all of the experiments discussed in this paper, a pair of small and weak axisymmetric vortices are placed at various separation distances, d, at the 15°N latitude. The separation distance varies from 640 km to 1440 km in different experiments.

The atmospheric environmental conditions are set to provide rapid development of the initial vortices into tropical storms. In particular, relative humidity in the lower 2-km layer is set at 95%. The *Jordan* [1958] mean vertical temperature profile typical of the tropical atmosphere in August is used initially, with the sea surface temperature (SST) set to 28°C.

In most numerical experiments the initialization of the vortices' circulation is conducted by setting temperature perturbation at t=0 as

$$T(r,z) = \frac{1}{2} T_m(z) \left[1 + \cos\left(\frac{\pi}{2} r/r_m\right)\right] \quad r \le 2r_m$$
$$T(r,z) = 0 \quad r > 2r_m \qquad (1)$$

where $T_m(z)$ is the vertical profile of temperature deviation from its background value at the vortex axis. The temperature anomaly at the vortex axis $T_m(z)$ increases linearly with height from 0 K at level $\sigma = 11/12$ to its maximum (usually 3 K) at $\sigma = 2/6$ and then decreases to 0 K at $\sigma = 1/6$. Changing this maximum value varied the intensity of the initial vortices. The parameter r_m determines the horizontal scale of the vortices. It corresponds to the maximum horizontal temperature gradient and is equal to the radius of maximum winds of the initial vortices. According to (1), the temperature deviation has a maximum at the axis of the vortices, decreases to half its maximum value at $r = r_m$ and attains zero at $r = 2r_m$. Initial pressure and tangential velocity fields were calculated from (1) using the static and gradient wind balance equations.

In the coupled tropical cyclone-ocean experiments the ocean is assumed to be horizontally homogeneous and quiescent. For most

Table 1. Summary of Experiments

Experiment	West Vortex ΔT_{9km}, °C	West Vortex Pressure, mbar	West Vortex V_{max}, m/s	East Vortex ΔT_{9km}, °C	East Vortex Pressure, mbar	East Vortex V_{max}, m/s	Interaction Regime
A-640	3.0	987.3	26.9	3.0	987.3	26.9	Partial Merger
AV-640W	3.5	985.6	28.9	3.0	987.3	26.9	Mutual Straining Out
AV-640E	3.0	987.3	26.9	3.5	985.6	28.9	Mutual Straining Out
AOV-640E	3.0	987.3	26.9	3.5	985.6	28.9	Mutual Straining Out
AV-800W	3.5	985.6	28.9	3.0	987.3	26.9	Partial Merger
AV-800E	3.0	987.3	26.9	3.5	985.6	28.9	Mutual Straining Out
AOV-800W	3.5	985.6	28.9	3.0	987.3	26.9	Mutual Straining Out
AOV-800E	3.0	987.3	26.9	3.5	985.6	28.9	Mutual Straining Out
CAV-800E	3.0	987.3	26.9	3.5	985.6	28.9	Complete Merger
AGV-800W	6.0	977.0	37.6	3.0	987.3	26.9	Straining Out
A-1440	3.0	987.3	26.9	3.0	987.3	26.9	Elastic Interaction
AO-1440	3.0	987.3	26.9	3.0	987.3	26.9	Elastic Interaction

The experiments with fixed in time SSTs are denoted by the letter A (atmosphere only). In the experiments denoted by the additional letter V (Velocity), the initial vortices have different intensities. The letters W (west) and E (east) indicate which vortex in the pair is set stronger (or larger) initially. Experiments additionally denoted by the letter C (CISK) indicate those in which a CISK-type parameterization of cumulus convection is utilized. The letter O (ocean) denotes the experiments in which coupling with the ocean was taken into account. The symbol G (gradient) denotes the experiments with a gradual decrease of the SST to the north, beginning with 15°N with a gradient of 1°C/800 km.

of the western Pacific the mixed layer depth varies from 25 m to 55 m during a tropical cyclone season, according to the *Levitus* [1982] ocean climate atlas. For our idealized experiments we have chosen to use an average value of 40 m.

A list of the experiments conducted is presented in Table 1. The experiments with fixed in time SSTs are denoted by the letter A (atmosphere only). In the experiments denoted by the additional letter V (velocity), the initial vortices have different intensities. The stronger (weaker) vortex was initialized by an increase (decrease) of the maximum T_m by 0.5 K as compared to the basic value of 3 K. The numbers denote separation distance (in kilometers) between initial vortices. The letters W (west) and E (east) indicate which vortex in the pair is set stronger (or larger) initially. Note that in our experiments more intense storms were usually stronger and larger. Experiments additionally denoted by the letter C (CISK) indicate those in which a CISK-type parameterization of cumulus convection is utilized. The letter O (ocean) denotes the experiments in which coupling with the ocean was taken into account. The symbol G (gradient) denotes the experiment with a gradual decrease of the SST to the north, beginning with 15°N with a gradient of 1°C/800 km.

In most of the experiments the binary storms began to intensify when the effect of their interaction was negligible. The mutual interaction influenced storm development when they reached the tropical cyclone strength. Typically, at the beginning of the interaction, the model storms had well-developed tropical cyclone (TC) structures with warm core temperature anomalies exceeding of 15°C at σ = 2/6 level. Vertical cross sections of radial and tangential velocities, as well as vorticity at t = 6 hours (weak vortices) and 48 hours (developed TC) are shown in Figures 1a and 1b, respectively. At t = 48 hours the maximum of the tangential velocity was 45 m/s, and the maximum of the radial velocity in the boundary layer reached 19 m/s. The vorticity was positive in the central area with the radius of about 120 km. The maximum of tangential velocity is located at σ = 5/6 at t = 6 hours and at σ = 4/6 at t = 48 hours. At t = 6 hours the level σ = 5/6 corresponds to a height of about 1600 m above the surface. At t = 48 hours the level of σ = 4/6 corresponds to a height of about 3 km above the surface. So, in both cases, maximum of tangential wind is located in the vicinity of the top of the boundary layer. To the best of our knowledge, there are no reliable data concerning heights of the tangential velocity maximum in very intense tropical cyclones with the minimum surface pressure as low as 930 hPa. One can expect, however, an increase of the depth of the boundary layer with an increase in the tangential velocity. Some overestimation of the height in the model is possible however due to the relatively low vertical resolution used.

4. Regimes of Binary Storm Interaction

In this section we discuss different regimes of binary storm interactions found in the experiments performed in this study. When describing these regimes, we will use the following terminology that is partially based on that of *Dritschel and Waugh* [1992]:

1. Complete merger (CM) is the coalescence of the storms into a single storm without any loss of their vorticity into the surrounding environment.
2. Partial merger (PM) defines the interaction when one of the storms is only partially entrained and captured by the opposite storm.
3. Straining out (SO) occurs when the weaker storm is destroyed by the stronger one at some separation distance.
4. Mutual straining out (MSO) occurs when both storms are stretched out and weaken at some separation distances. At some separation distance the storm approach can be replaced by storm repulsion.
5. Elastic interaction (EI) occurs when the storms interact without any significant changes in their intensity and structure.

The specific regimes of binary storm interactions in experiments discussed below are presented in Table 1. Below we illustrate and discuss some of the most important features of these regimes.

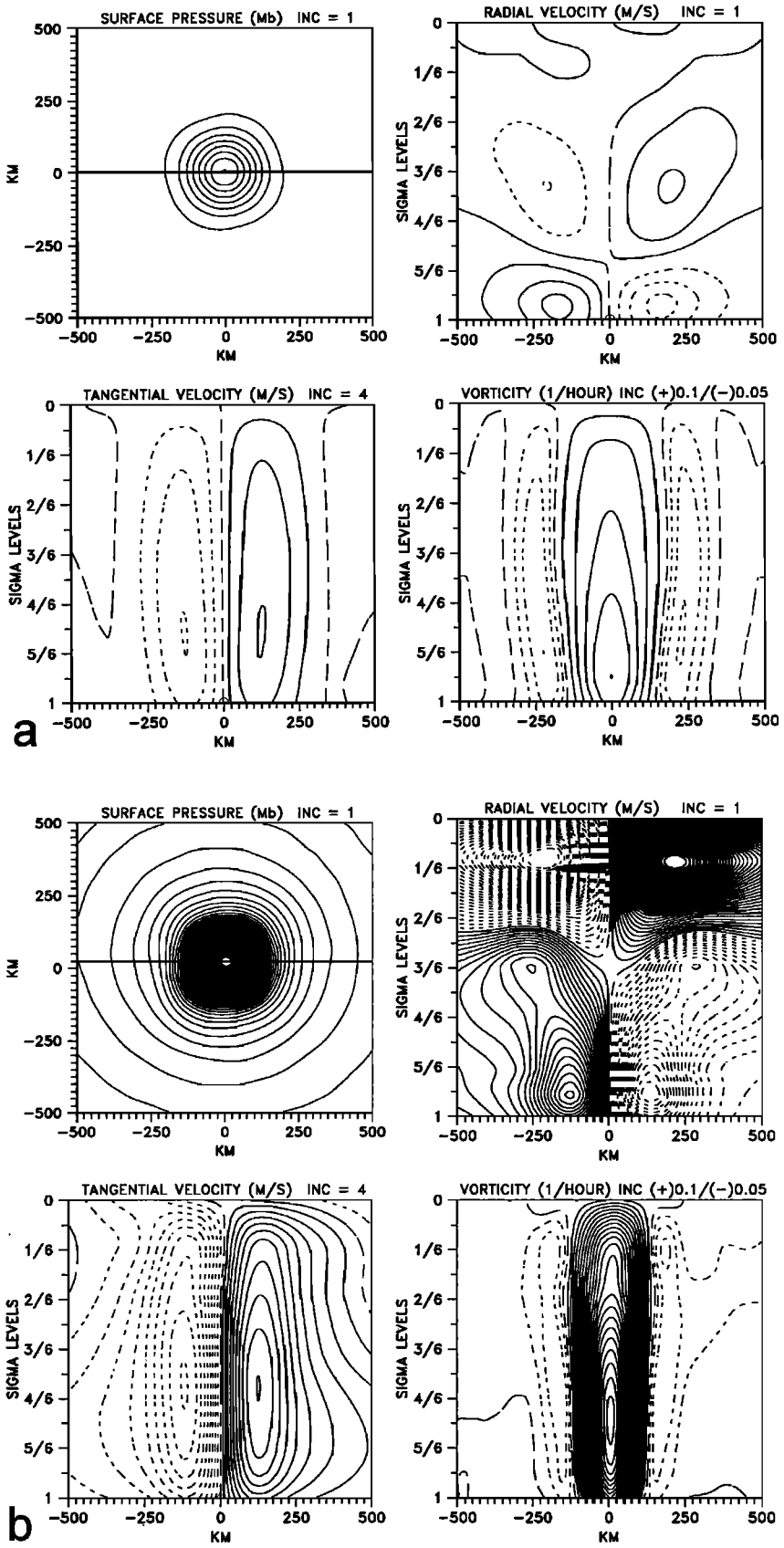

Figure 1. Vertical cross sections of the radial and tangential velocities and the vorticity at (a) t=6 hours (weak vortices) and (b) at t=48 hours (developed tropical cyclone(TC)). Solid lines denote positive values, dashed lines denote negative values. Increments between the vorticity contours are 0.1 h^{-1} for positive values and 0.05 h^{-1} for negative values (dashed lines). INC denotes increment.

4.1. Complete and Partial Merger

As follows from the experiments discussed in this paper, as well as from supplemental numerical experiments with separation distances of a few hundred kilometers, CM was observed when the initial separation distances were smaller than 400 km and in the cases when one of the storms was significantly weaker than its counterpart. The regime of CM is illustrated by FKG and *Wang and Holland* [1995] in detail, and therefore we only briefly outline its main features here. Since at small separation distances the radial velocities of the stronger storm are large, the merger is mostly caused by advecting the weaker storm into the circulation of the stronger one by the radial velocity component, similar to the effect of cloud merger studied by *Kogan and Shapiro* [1996]. Indeed, radial velocities in a mature storm may exceed 4 m/s at distances as large as 400 km from the storm center (Figure 1). Thus the central zone of one storm turns out to be embedded into the radial "background" flow created by its counterpart. Advection of the vorticity in one storm by the tangential circulation of the opposite storm may also contribute to storm attraction and merger because of the positive vorticity between the storms, as suggested by FKG. Note that development of tropical storms at distances of 400 km and less is hardly possible. However, entrainment of cloud clusters and weak mesoscale convective systems into a tropical storm is a regularly observed phenomenon in the western Pacific. Entrainment of weak convective mesoscale disturbances into stronger ones is an important factor of TC genesis [e.g., *Simpson et al.*, 1997]

We observed PM regime in A-640 when two initially weak and equal vortices were separated by 640 km (Table 1). Storm interaction in this experiment is illustrated in Figures 2 – 4. After about a 24-hour transition period, both storms rapidly intensified, but the storm initially located to the west (storm W) remained more intense for the entire integration period. After about 72 hours the intensity of the opposite storm, initially located to the east (storm E), leveled off, and by 96 hours the difference in the central pressures reached 40 mbar. Shortly after that, the weaker storm lost its identity in the pressure field (Figure 2).

The intensity changes in this experiment can be attributed to the following. Mutual interaction began when both storms were located at nearly the same latitude of about 15°N. It resulted in a northward acceleration of storm E (transported by the tangential circulation of storm W) and hindered northward movement of

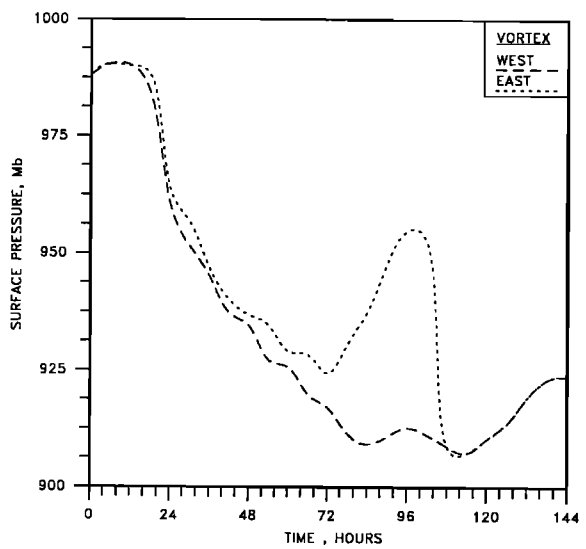

Figure 2. Time series of minimum sea surface pressures in binary storms in A-640.

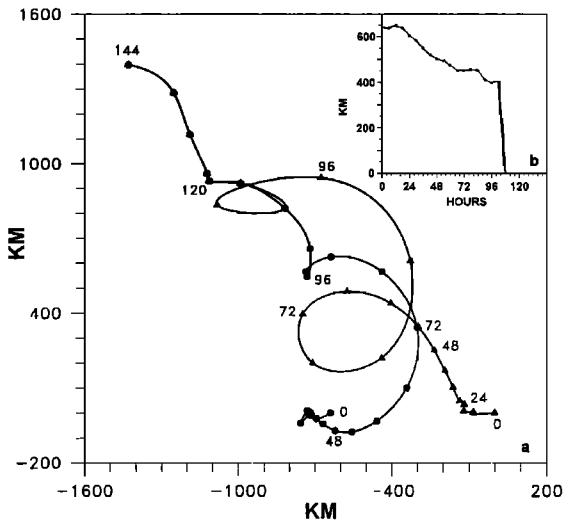

Figure 3. (a) Tracks of the storms in A-640; (b) time dependence of separation distance between the storm centers.

storm W (because of the southward tangential velocity of storm E). As a result, storm W moves with lower speed, and in the case of no ocean coupling (or weak coupling) this storm has an advantage in the development rate compared to its counterpart (FKG). Typically, a faster moving storm experiences a larger vertical wind shear because in the vicinity of the surface any speed, including the translation one, is small (or zero), while at higher levels the translation speed is large. An Increase in the vertical shear is known to impede the development of a TC [*Gray*, 1978]. Another possible cause of the difference in the storm development rates is due to faster increase of the Coriolis parameter for storm E as compared to storm W. As was shown numerically by *Khain* [1984] and *Ivanov and Khain* [1983], an increase in the latitude above 15°N tends to retard TC development. Conceptually, this can be inferred from the equation of the gradient wind balance

$$\frac{1}{\rho}\frac{\partial p}{\partial r} = \frac{V^2}{r} + fV , \qquad (2)$$

where p is the pressure, V is the tangential velocity, and r is the distance from the storm center. For the pressure gradient being given, the higher value of the Coriolis parameter corresponds to lower tangential wind V. Thus northward movement of a TC requires an increase in the pressure gradient for keeping the wind velocity unchanged.

During their interaction the storms followed converging trajectories accompanied by mutual orbiting (Figure 3). Evolution of the low-level vorticity (σ=5/6) in this experiment is shown in Figure 4. At 78 hours, while both storms were intense and close to axisymmetric, entrainment of the weaker storm into the circulation of the stronger one began. The mutual approach led to rapid development of differences in their intensities and sizes. This process was accompanied by stretching and breaking up the vorticity field of the weaker storm. The vertical shear of the tangential circulation of storm W (a decrease of the tangential velocity with height) caused weakening of its counterpart and its rapid filing (Figure 2). This is because the tangential velocity of storm W serves as a "background" flow for storm E, causing the lower layers of storm E to be advected faster than the upper layers. Thus storm E was stretched out by the circulation of storm W not only in the horizontal plane but also in the vertical. Some idea about the magnitude of the vertical shear can be derived from Figure 1b, where the tangential velocity is shown.

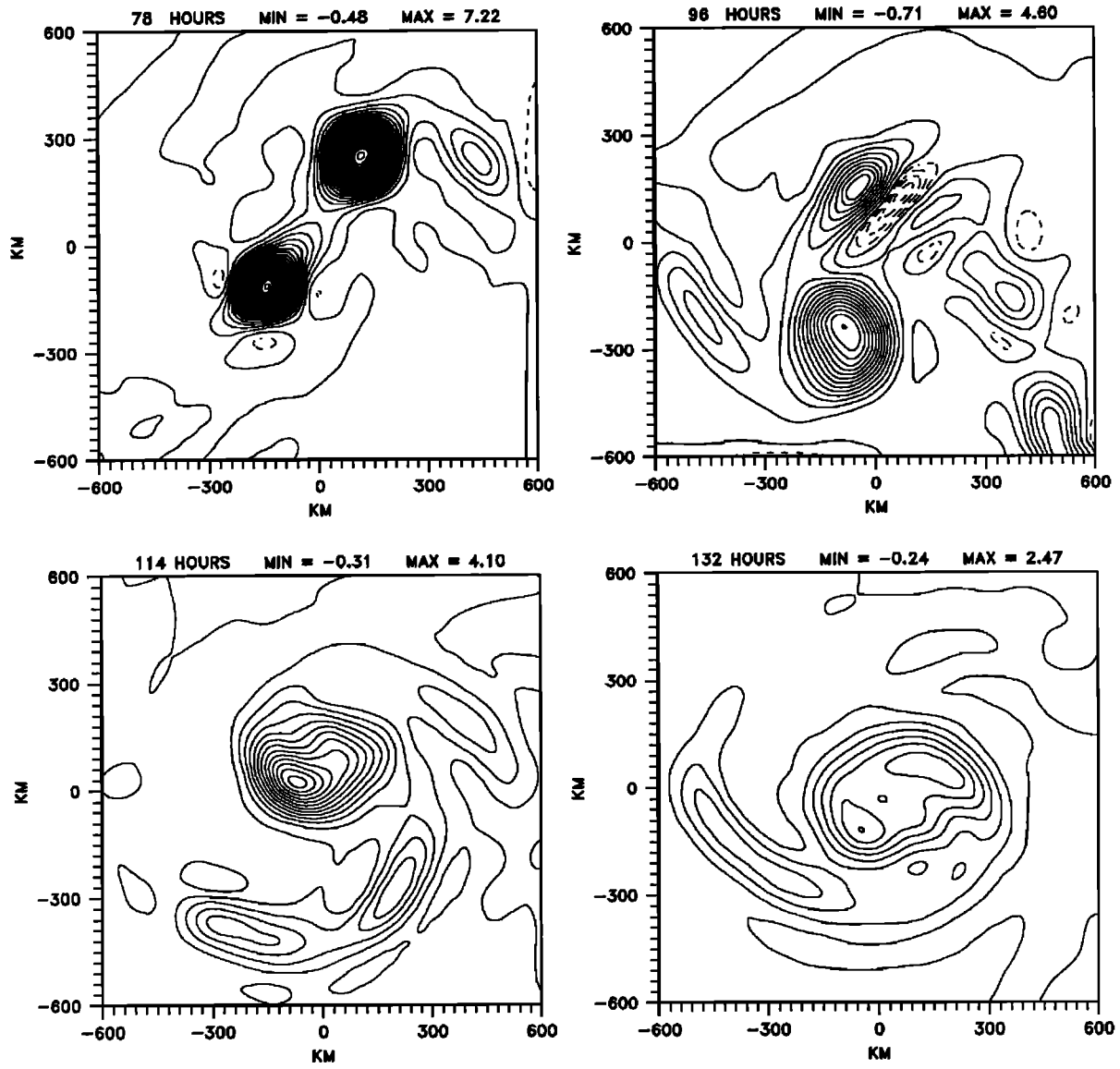

Figure 4. Vorticity field (h^{-1}) in the lower troposphere ($\sigma\sigma$ = 5/6) at different times in A-640. Increments between the vorticity contours are 0.3 h^{-1} for positive values (solid lines) and 0.15 h^{-1} for negative values (dashed lines).

While the weaker storm continued to be entrained into the stronger one, a detachment of vorticity patches occurred after 84 hours, clearly seen at 96 hours in Figure 4. At about 132 hours a large single storm was formed. Remnants of the weaker storm turned into vorticity of the winner storm, which may be interpreted as rainbands. Note that the timing of merger is more accurately identified from the vorticity fields than from the pressure field. As seen in Figure 2, the weaker storm lost its identity in the pressure field much earlier, at about 100 hours. Thus the timing is more accurately identified from the vorticity field. This is because surface pressure gradients in the stronger storm exceed those in the weaker storm at a significant distance, say 200 km, from its center. This means that the weaker storm is difficult to detect within the pressure field of the stronger one at this distance. The weaker storm will be identified by only a small distortion of isobars of the pressure field of the stronger storm. On the other hand, the vorticity within the weaker storm can be readily identified in the background of the vorticity field of the stronger storm. This is because of a rapid decrease of the vorticity with distance in the stronger storm and a significant value of maximum vorticity in the vicinity of the center of the weaker storm. The storm that was formed after the merger had a fairly large size with a 120–km radius eye.

4.2. Straining Out

This type of interaction occurred when the difference in the intensity and size of the binary storms was significant. Supplemental numerical experiments indicated no sharp transition between PM and SO. We found that the greater the difference in storm strengths and the larger the separation distance were, the larger the fraction of the vorticity related to the weaker storm that was radiated off and the smaller the fraction that was entrained into the winner storm. "Radiation off" means the separation of the peripheral part of the vorticity field from the remaining vorticity of the stretched storm and its propagation out of the computational region. When the difference in the storm strengths was set to be very significant as, for example, in AGV-800W (Table 1), the weaker storm was stretched and destroyed at a distance of about 500 km, without advecting its vorticity into

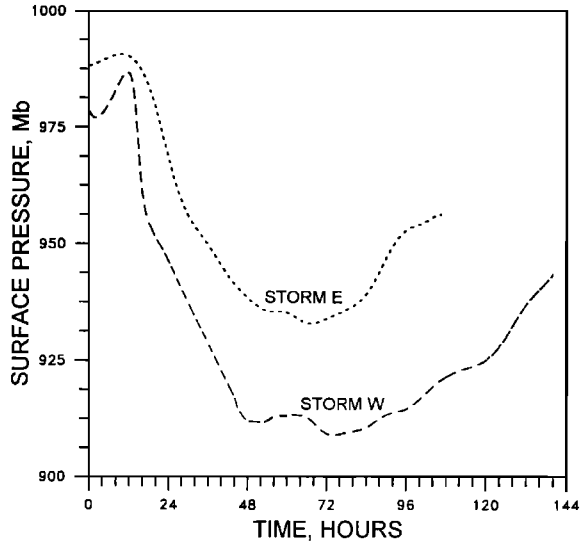

Figure 5. Time series of minimum sea surface pressure in the storms in AGV-800W.

the winner storm. In this experiment the maximum deviation of temperature in the stronger vortex was initially set at 3 K higher than in the weaker one. The time dependence of the minimum sea surface pressure and the sea surface pressure field in this experiment are shown in Figures 5 and 6 respectively. When stretching of the weaker storm began, the difference in sea surface pressure minima reached about 50 mbar (Figure 5). At 84 hours, the weaker storm was fairly compact and quasi-symmetric. However, during the following 12 hours, the weaker storm approached closer to the stronger one and was stretched out, was temporarily transformed into a rainband of the stronger storm, and then finally disappeared in the pressure field (Figure 6). The process of stretching is illustrated in more detail in Figure 7, where the vorticity field in the lower troposphere (σ=5/6) at different times is presented. One can see that each act of stretching is accompanied by a breakdown of the vorticity field of the weaker storm and radiation of the broken part off. The latter means a separation of the peripheral part of the vorticity field from the remaining vorticity of the stretched storm. Formation of three local maxima in the weaker storm vorticity field is clearly seen at 120 hours.

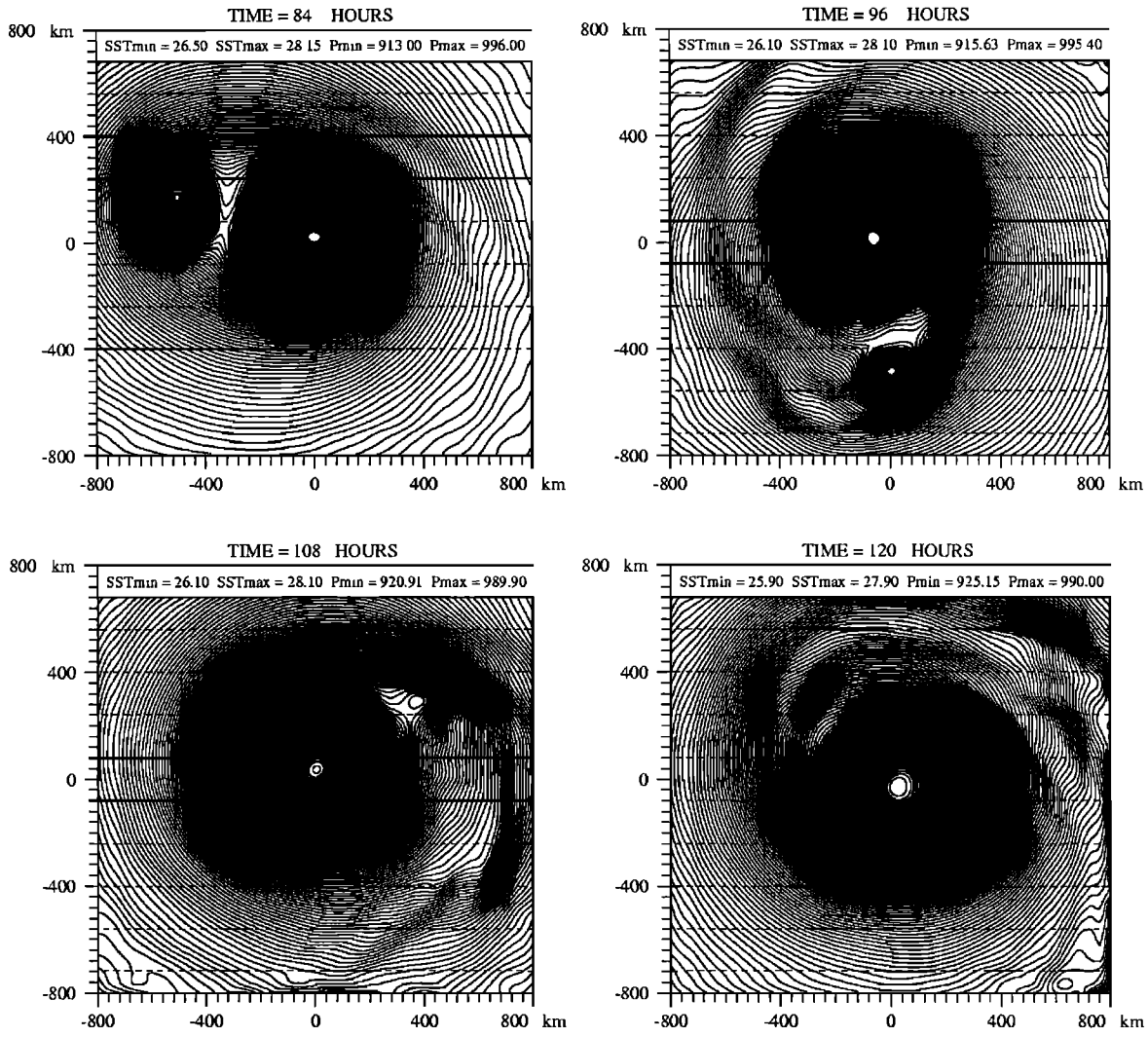

Figure 6. Sea surface pressure fields in AGV-800W at different times, shown with an increment of 0.5 mbar. Stretching of the weaker storm is clearly seen.

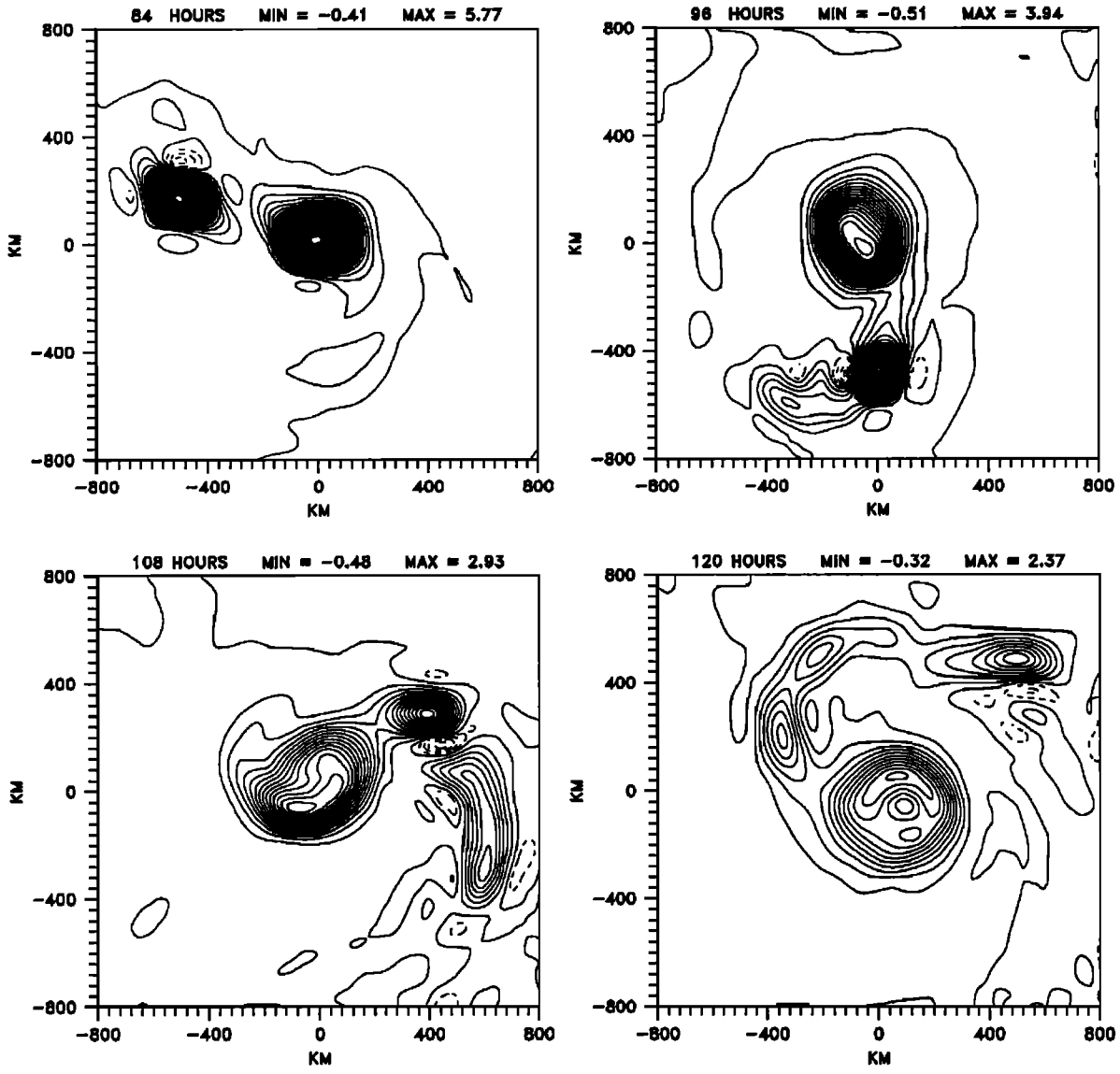

Figure 7. Vorticity field (h^{-1}) in the lower troposphere (σ = 5/6) at different times in AGV-800W. Increments between the vorticity contours are 0.2 h^{-1} for positive values (solid lines) and 0.1 h^{-1} for negative values (dashed lines). One can see that the process of stretching consists of several acts of breaking down of the weaker storm vorticity.

4.3. Mutual Straining Out

In the majority of the experiments conducted with initial separations ranging between 650 and 1000 km, MSO occurred. For an illustration of this process, we discuss here the binary storm interaction in AV-800E. Figure 8 shows the storm tracks and separation distance in this experiment. The characteristic feature of the storm interaction in this experiment is replacement of initial attraction and intensification of the storms by their repulsion and weakening. By 96 hours the separation distance reached its minimum value of 420 km and remained virtually unchanged up to 124 hours, but it rapidly increased after that (Figure 8b).

Similar to the experiments discussed above, mutual interaction in AV-800E led to weakening of storm E. After 40 hours its minimum surface pressure was consistently higher compared to that of storm W (Figure 9). Note that intensification of one storm is typically accompanied by weakening of its counterpart. We attribute this effect to increasing ability of the stronger storm to stretch out and suppress the development of its counterpart. The most pronounced effect of storm interaction on the storm intensities began at about 84 hours, when the separation distance decreased to about 500 km.

Figures 10 and 11 show the evolution of the low-level (σ = 5/6) vorticity, and the middle atmosphere (σ = 0.5) vertical p velocity fields from 72 hours to 108 hours is shown. The changes of the storm structures are evidently more conspicuous in the vertical velocity fields. This is because the vertical velocity is induced by the flow divergence that is very sensitive to the changes in the radial velocity field. At 72 hours, both storms were fairly compact. The beginning of the mutual stretching is clearly seen about 12 hours later. The mutual stretching leads to formation of enhanced vertical velocity and vorticity bands located in the rear of the moving storms, at their most remote distances from each other. The vorticity field becomes elongated in the direction of the line between the storm centers. The radial shears in both the tangential and radial velocities in each storm cause stretching, the rainband formation, and their radiation off.

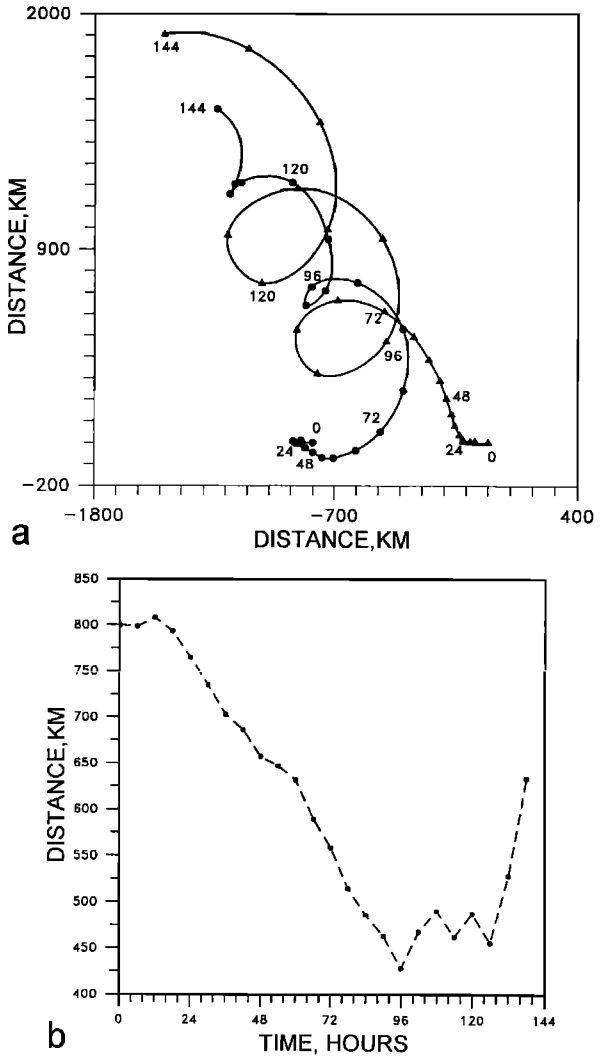

Figure 8. (a) Tracks of the storms in AV-800E; (b) time dependence of separation distance between the storm centers.

Another interesting feature we find in AV-800E is that the maxima of the vertical updrafts (and correspondingly the maxima of convective heating) appear on the opposite, most remote sides of the storms. This effect can be seen from comparison of Figures 10 and 11. The shift is pronounced already at 72 hours (Figure11), when the storms are still rather compact. However, the most pronounced asymmetry in the vertical velocity field appears to be during the mutual stretching (e.g., 96 hours), when the vertical velocities between the storm centers are much smaller than the strong vertical updrafts on the remote sides of the storms. A clear displacement of the vertical updrafts from the storm centers can be seen by comparing their location with the location of the vorticity maxima, which can be referred to as the storm centers.

This characteristic feature was observed in other experiments as well and may be explained as follows. From Figure 1b one can see that the maximum of the radial velocity in the upper troposphere is reached at about 200 km from the storm center. At larger distances the radial velocity decreases, indicating the air descent. Thus a storm approaching from a distance of a few hundred kilometers experiences descending circulation created by its counterpart.

At radii exceeding 200 km the value of subsidence caused by one storm decreases with an increase in the distance to the storm axis. That is why the subsidence caused by one storm affects the vertical velocity of its counterpart mainly between the interacting storms and actually does not affect vertical velocities on its remote side. Thus the superposition of ascending and descending motions of interacting storms induces an asymmetry in the field of the vertical velocity around interacting storms with the maximum updrafts at the opposite most remote sides of interacting storms.

This asymmetry leads to a corresponding redistribution of convective heating within the storms, which in its turn leads, supposedly, to a subsequent growth of the asymmetry of the vertical velocity field because of the existence of a positive feedback between values of the vertical velocity and the rate of convective heating.

We speculate that the main reason why the mutual approach in AV-800E was replaced by repulsion after 120 hours (Figure 8b) is related to the tendency of tropical cyclones to displace toward the areas of maximum heating [e.g., *Khain and Ginis*, 1991; *Willoughby, and Chelmow*, 1982; FKG], which in our case coincide with the areas of maximum vertical velocities. This is because vertical updrafts transport water vapor from lower levels along the moist adiabat. This is a characteristic feature of the explicit convection parameterization used in the model [see FKG; *Falkovich et al*,, 1995b].

This assumption is further supported by the results of the experiments with the CISK-type convective parameterization discussed below. Note that during their movement away from each other, the storms in AV-800E continued to weaken (Figure 9) due to mutual stretching.

Thus this experiment demonstrates that initial attraction and intensification of binary storms can be replaced by their repulsion and weakening. This type of storm interaction is consistent with observations of tropical cyclone interactions in the western Pacific [*Lander and Holland*, 1993].

4.4. Elastic Interaction

When the binary storms were separated at very large distances (greater than 1100 km) EI was observed. We illustrate this regime by considering the experiment A-1440 (Table 1). Figure 12 shows the storm tracks in A-1440. During the first 144 hours of integration, both storms moved primarily northward, but the translation speed of storm W was about 2 times smaller than the corresponding speed of storm E. The dominance of the northward

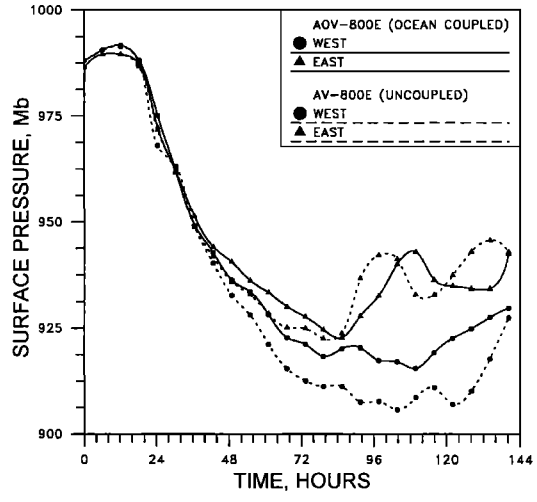

Figure 9. Time series of minimum sea surface pressures in the storms in AV-800E and AOV-800E.

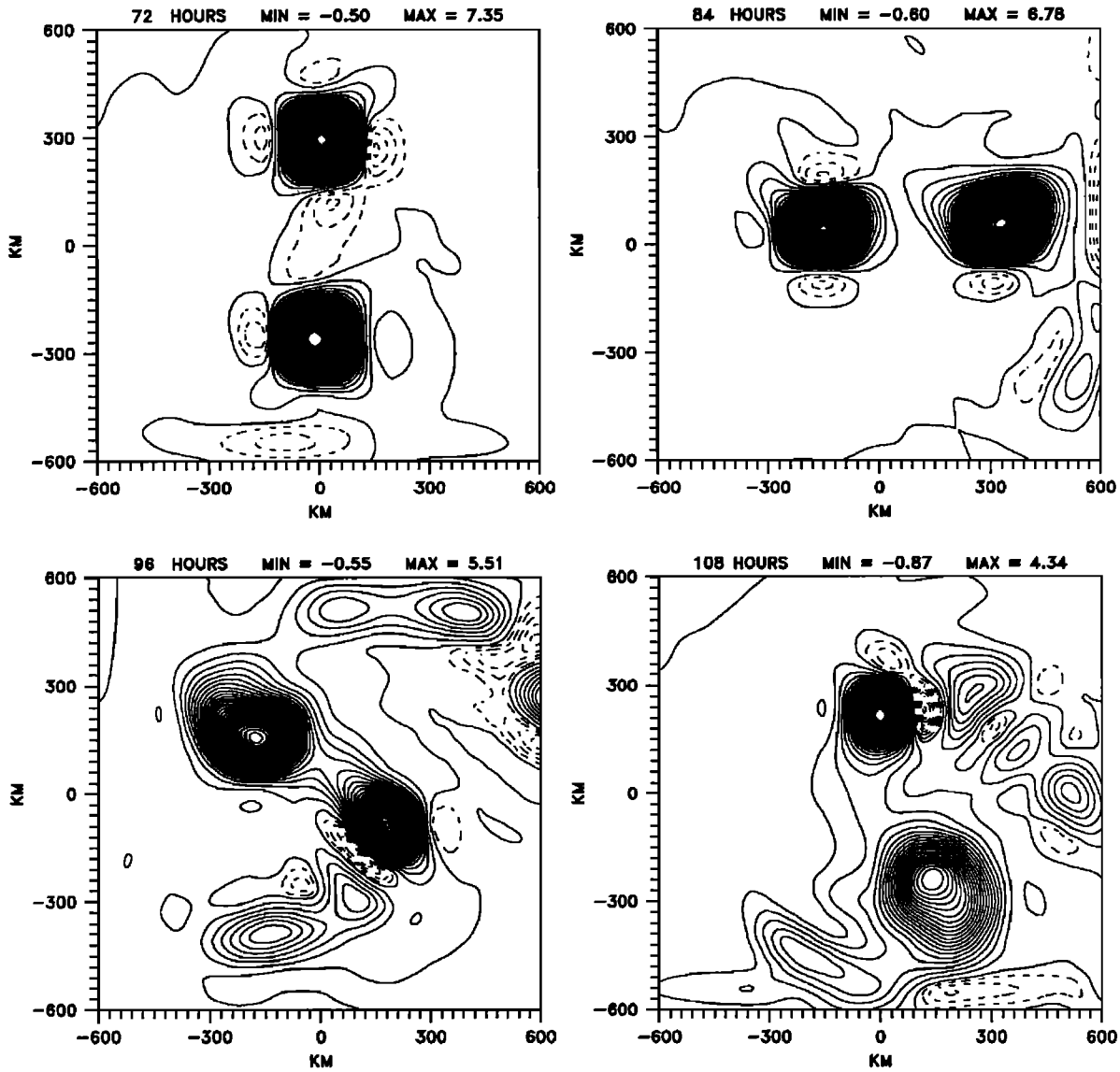

Figure 10. The low-level (σ = 5/6) vorticity fields (h^{-1}) from 72 hours to 108 hours in AV-800E. Increments between the vorticity contours are 0.2 h^{-1} for positive values (solid lines) and 0.1 h^{-1} for negative values (dashed lines).

movement and the difference in the speeds are clearly caused by storm interaction. The movement of each storm is primarily determined by a vector sum of the several forces. First, both storms tend to move northwest due to the beta effect. Second, the tangential velocity of storm W (E) forces storm E (W) to move north-northwest (south-southeast). Finally, the storms are pushed away from each other due to the negative vorticity between them (FKG). The net force drives each storm northward, but this force is apparently weaker for storm W. The northward movement of binary barotropic vortices was also observed by *Chan and Law* [1995] when the separation distance was significantly greater than the storm sizes. Both storms had nearly the same intensity over the entire integration period: The maximum differences in central pressures never exceeded more than 5 mbar (not shown). Moreover, the time evolution of the minimum surface pressure for each storm was very similar to that in an analogous single-storm run. Thus the binary interaction did not actually influence the storm intensities in this case. No apparent vorticity exchanges between the storms were observed either in this case, so the vorticity structures of both storms were preserved over the entire period of their interaction.

5. Sensitivity Experiments

In this section we discuss the results of various sensitivity experiments conducted to investigate the effects of convective parameterization, ocean coupling, initial size of the vortices in the pair, and separation distance on the regime of binary storm interaction.

5.1. Role of Convective Parameterization

We first investigate the role of convective parameterization in simulations of binary storm interaction with baroclinic models. Two methods will be compared: calculation of latent heat on resolvable scales as described in section 2 and a CISK-type parameterization with the heating function proportional to the low-level vorticity as used in the simulations of *Wang and Holland* [1995]. Note that *Chang* [1983] also used a prescribed heating function for convection parameterization.

We have conducted a set of experiments with the CISK-type parameterization used by *Wang and Holland* [1995] (hereafter

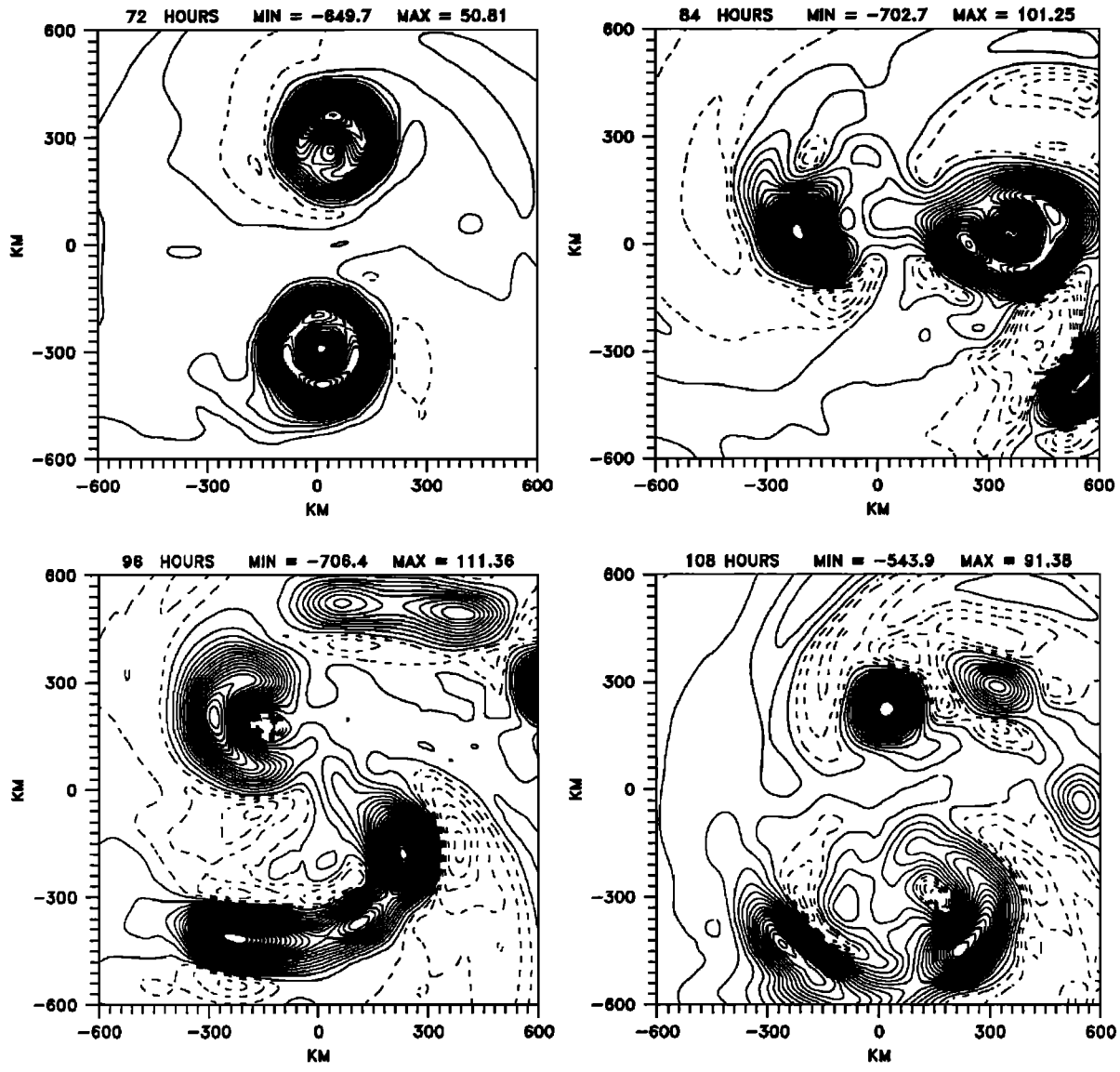

Figure 11. The middle atmosphere ($\sigma = 0.5$) vertical velocity (mbar/h) fields from 72 hours to 108 hours in AV-800E. Increments between contours are 30 mbar/h for negative values (updrafts, solid lines) and 15 mbar/h for positive values (subsidence, dashed lines).

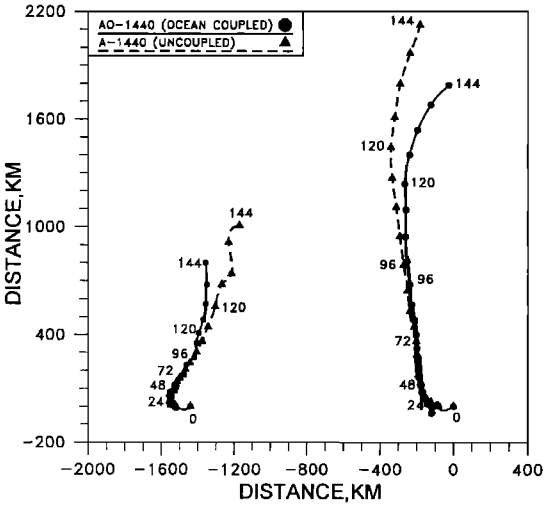

Figure 12. The storm tracks in A-1440 and AO-1440.

CISK experiments). In these experiments the heating function $Q(\sigma)$ is determined by low-level vorticity $\zeta(\sigma = 5/6)$:

$$Q(\sigma) = \alpha \sin(\pi\sigma) \exp(-\delta\sigma) \quad \zeta_{\sigma=0.9}, \; r < 400 \text{ km} \tag{3}$$

$$Q(\sigma) = 0, \qquad \zeta_{\sigma=0.9} < 0, \; r > 400 \text{ km},$$

where σ is the sigma level and α and δ are the parameters which define the scale and shape of the heating function.

Here we consider the results of one experiment, CAV-800E (Table 1), as an example. This experiment is analogous to AV-800E except for using the CISK parameterization (3). The parameters α and δ were chosen in such a way that the intensities of the storms in CAV-800E were close to those in AV-800E. Nevertheless, dramatic differences in the storm interaction regimes were observed. In CAV-800E the separation distance decreased monotonically and resulted in complete merger (CM) at 90 hours. We should note that in all supplemental CISK experiments performed, CM took place, including those with either equal or unequal initial vortices (not shown).

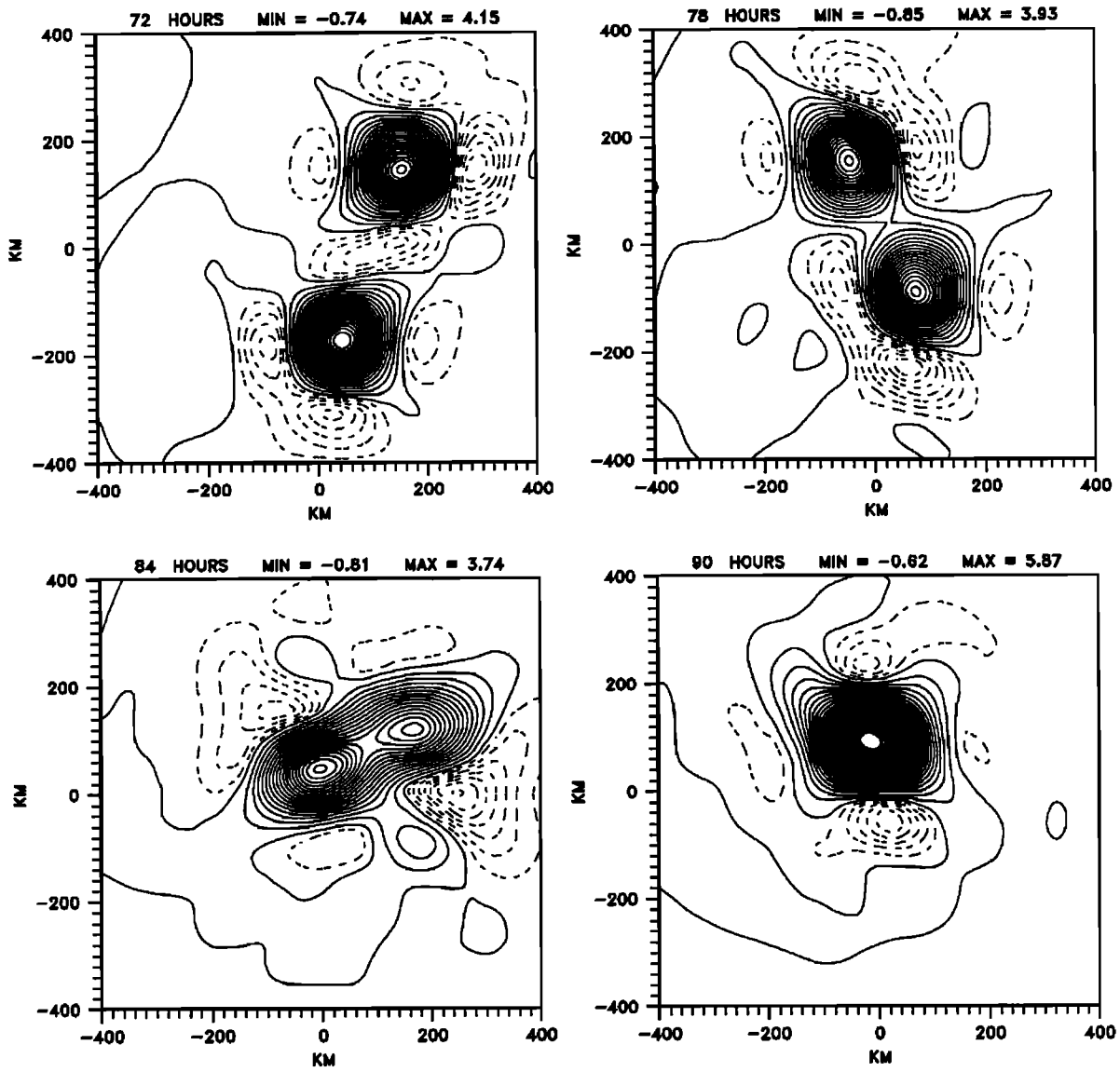

Figure 13. The low-level (σ = 5/6) vorticity fields from 72 hours to 90 hours in CAV-800E. Increments between the vorticity contours are 0.2 h^{-1} for positive values (solid lines) and 0.1 h^{-1} for negative values (dashed lines).

The process of storm merger in CAV-800E is shown in Figures 13 and 14, where the low-level vorticity (σ = 5/6) and middle atmosphere (σ = 0.5) p vertical velocity are presented. One can see that the merger takes place with no any noticeable distortions in these fields. This is very different from what we observed in the experiments in which the latent heat release was calculated on resolvable scales.

To illustrate the difference in the structure of the interacting storms in AV-800E and CAV-800E, we present Figures 15a and 15b, which show the contours of the low-level vorticity, as well as vertical sections of the vorticity in these experiments. One can see (Figure 15a) that both storms in CAV-800E were very compact. That allowed them to approach each other to small distances where their corresponding radial velocities were relatively large. As a result, the attraction was accelerated due to increased advection of one storm by the radial circulation of the other during the storm approach. Noticeable persistence of storm circulation in the CISK experiments can be explained as follows. The latent heat release in the experiments with a CISK-type parameterization is proportional to the vorticity at the top of the boundary layer at r < 400 km. At larger radii, no heating is assumed. The vorticity has a maximum in the center of the storm and rapidly decreases with the increase of the distance from the storm center. The low-level vorticity is determined by the pressure field (through the equation of gradient balance), which is close to axisymmetric. As a result, the maximum of convective heating in these experiments is located at the vertical axis passing through the point of the low-level vorticity maximum, usually coinciding with the surface pressure minimum. The heating rapidly decreases with the distance from the storm center, resulting in the compact storms observed in the CISK experiments. Being dependent on only the vorticity structure in the boundary layer, the heating is actually not affected by the vertical (or horizontal) wind shears induced by the other storm (see formula(3)), because this shear is mainly above the boundary layer top (see Figure 1). It is speculated that the positive feedback (the symmetric vorticity causing symmetric convective heating causing symmetric pressure causing symmetric vorticity) determines very stable and compact storm structures in the cases with the CISK-type convective parameterization. The vertical structure of the vorticity and vertical velocity of each storm remains actually unchanged during the storm attraction as it is not

sensitive to vertical and horizontal wind shears created by its counterpart. This explains why the regime of mutual straining out is never observed in these experiments.

When convective heating is determined by transport of water vapor, the latent heat release is largely dependent on the divergence field, which is not symmetric with respect to the storm center during the storm interaction. As demonstrated above, the updraft maxima are located at the opposite, most remote sides of the interacting storms. Correspondingly, the latent heat is also asymmetric. During storm interaction, the tangential circulation of one storm transports the water vapor of another one horizontally, leading to formation of rainbands, and thus spreading latent heat over a large area. As we discussed above, when one storm is embedded into a highly sheared flow of the opposite storm it loses its symmetric structure and weakens. Horizontal spreading of the convective heating affects the pressure and vorticity fields in AV-800E (Figure 15b), which is very different from what we observed in CAV-800E. The storm sizes in AV-800E were considerably larger and, therefore, mutual stretching began at significant separation distances.

When storms are separated at distances exceeding about 600 km, the mutual stretching processes are not effective. Therefore, despite the observed large differences in the character of storm interaction at distances smaller than 500 km, the separation distance at which the storms began to approach each other (mutual approach separation (MAS) in terminology of *Wang and Holland* [1995] was not very sensitive to convective parameterization and was about 1000 km. This value is similar to the one found by Wang and Holland.

5.2. Effect of Initial Storm Location

The experiments conducted also indicate that the type of binary storm interaction depends not only on the separation distance and their comparable strengths, but also on their mutual location. For example, in AV-800W, initial locations of the vortices were opposite to those in AV-800E. In AV-800W (AV-800E) storm W (storm E) was stronger, albeit the differences in intensities of the initial vortices were very small, about 2 mbar (Table 1). Nevertheless, even these small initial differences were

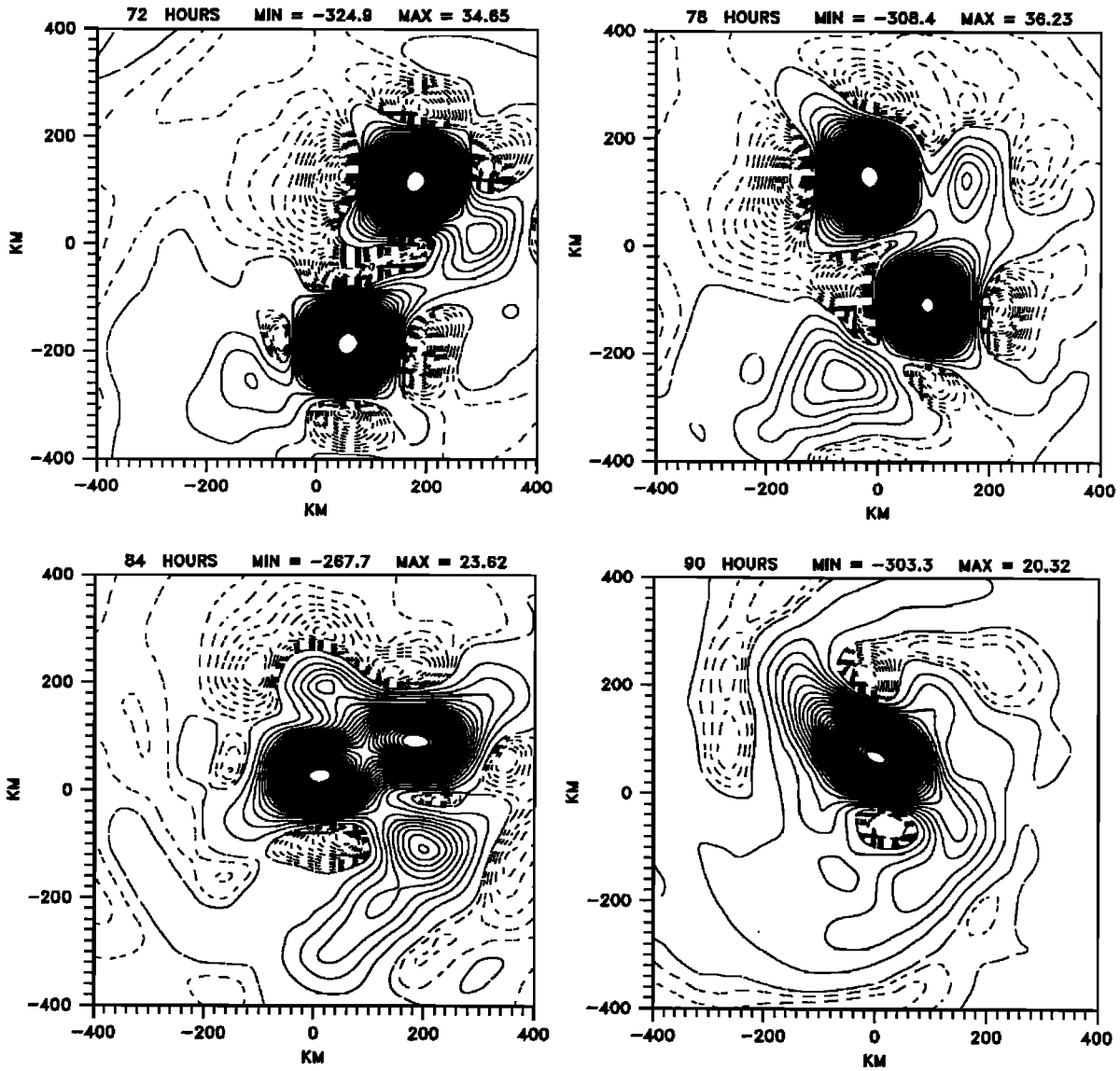

Figure 14. The middle-level ($\sigma = 0.5$) vertical velocity (mbar/h) fields from 72 hours to 90 hours in CAV-800E. Increments between contours are 10 mbar/h for negative values (updrafts, solid lines) and 2 mbar/h for positive values (subsidence, dashed lines).

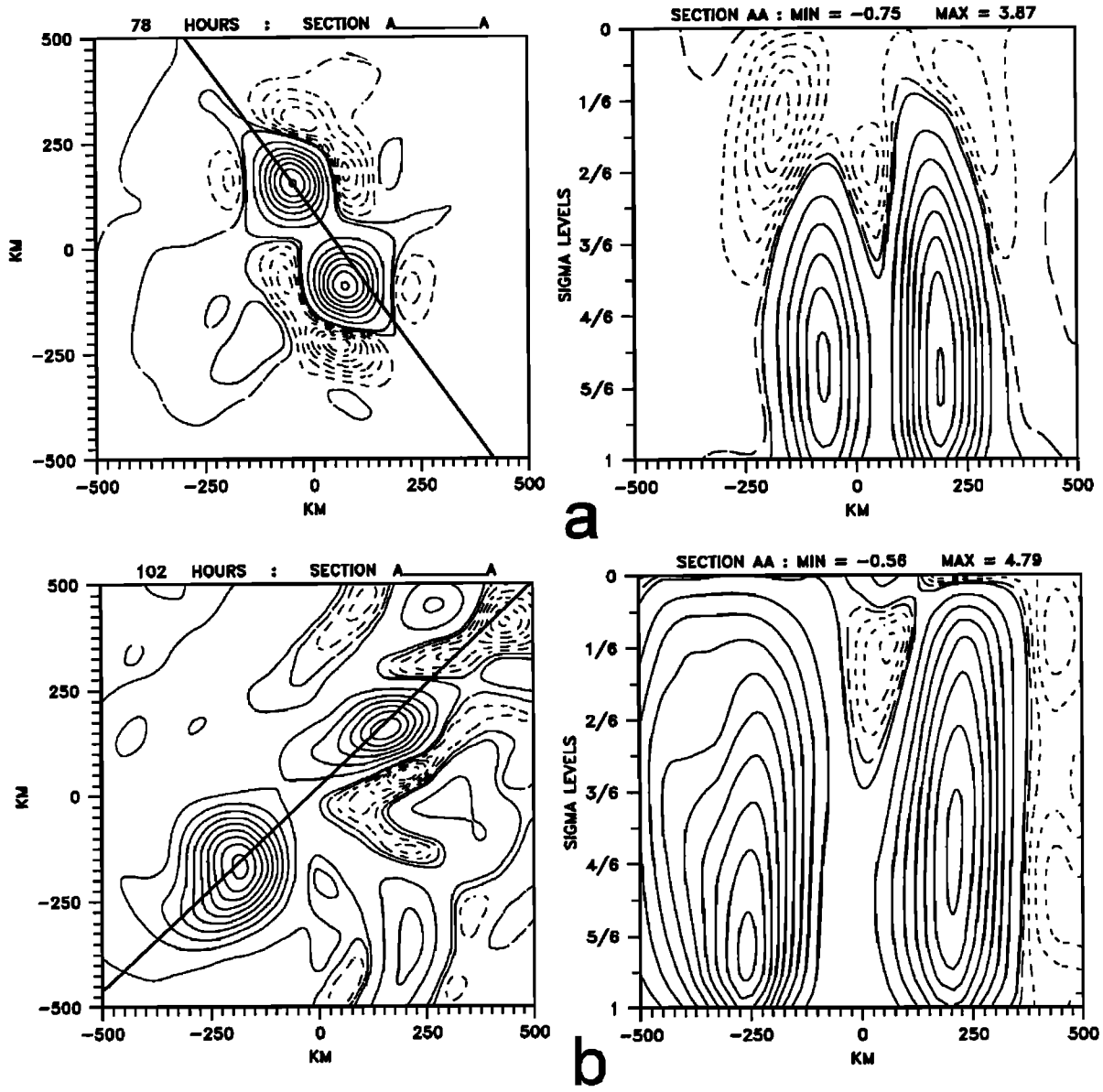

Figure 15. Contours of the vorticity at σ = 5/6 (left plots), as well as vertical cross sections (along the line connecting the storm centers) of the vorticity field (right plots) in (a) CAV-800E and (b) AV-800E. Increments between the vorticity contours are 0.5 h^{-1} for positive values (solid lines) and 0.1 h^{-1} for negative values (dashed lines).

sufficient to change the type of the storm interaction. MSO in AV-800E was replaced by PM in AV-800W, as is illustrated in Figure 16. In AV-800W the separation distance decreased monotonically to about 400 km, after which the weaker storm lost its identity in the pressure field of the stronger one.

5.3. Impact of the Ocean Coupling

In this section we discuss the role of ocean coupling on the regime of storm interaction. The tropical cyclone-ocean coupling is known to generate local SST decrease underneath the storm and may lead to its weakening [*Khain and Ginis*, 1991; *Ginis*, 1995]. As shown by FKG, ocean coupling can decrease the mutual orbiting velocity of each storm in the pair and thus significantly influences the storm tracks.

Our present experiments indicate that ocean coupling may also decrease the intensity of a stronger and slower moving storm more significantly than that of a faster moving and weaker storm. As a result, ocean coupling tends to decrease the difference in intensities of interacting storms and sometimes even determines the type of storm interaction.

The first effect is seen in Figure 17, where the storm tracks in AOV-800E (Table 1) are shown. This experiment is similar to AV-800E, except including the effect of ocean coupling. Comparison of the minimum pressures (Figure 9) shows that ocean coupling decreased the intensity of the stronger storm (storm W) in the storm pair. This is because storm W generated larger SST cooling that resulted in increased negative feedback of ocean coupling on the storm intensity. The intensities of the weaker storms (storms E) became very similar after 84 hours in both coupled and uncoupled experiments. We explain the effect as follows. In the uncoupled experiment, storm W was considerably stronger, which led to stronger suppression of the weaker storm E. In the coupled experiment, due to weakening of storm W, the influence of storm W on storm E was significantly reduced.

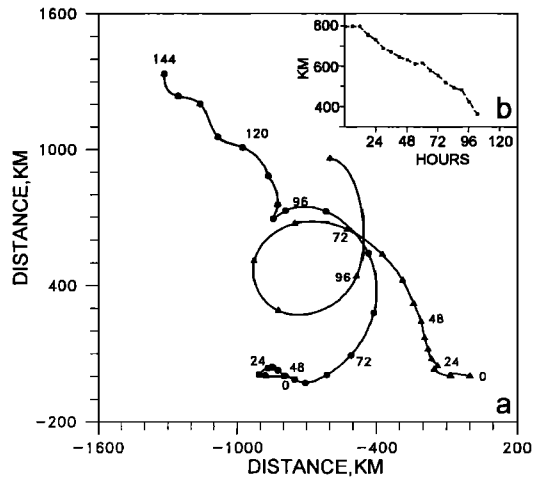

Figure 16. (a) Tracks of the storms in AV-800W; (b) time dependence of separation distance between the storm centers.

Figure 17a shows that the storms moved slower northward in AOV-800E and the distance between the storms is larger than in AV-800E. Storm attraction was replaced by repulsion in the coupled experiment when the separation distance reached 500 km, instead 420 km in the uncoupled experiment. We also observe the faster storm repulsion in AOV-800E as compared to that in AV-800E. We attribute this effect to the weaker radial advection associated with weaker storms in the coupled model. This assumption is supported by the results of a supplemental uncoupled experiment, which is similar to AV-800E, but in which SST was reduced from 28°C to 27°C. In this experiment the storms' behavior is similarly to that in AOV-800E.

Figure 18 shows the surface pressure and SST anomalies caused by tropical cyclone-ocean interaction in AOV-800E. The maximum SST decrease below each of the moving storms reached about 3°C. This value is typical for tropical cyclones moving with an average speed of 4-5 m/s [e.g., *Black and Shay*, 1995]. One can see that mutual orbiting led to weakening of the storm that crossed the cold wake created by its counterpart.

Supplemental experiments with different separation distances and mutual locations of initial vortices show that the ocean coupling may not only change the regime of interaction between storms, but also change the winner storm in case of partial merger regime.

For large separation distances as in AO-1440 the ocean coupling led to slower northward movement (Figure 12) mainly due to weaker intensities and smaller sizes of the storms. Note that while in the uncoupled experiment A-1440 storm W is stronger than storm E, in the coupled experiment, storm W turned out to be weaker (Figure 19) due to its slower motion and corresponding stronger SST cooling. Thus the ocean coupling may change the relative strengths of interacting storms even in a case when neither storm crosses the cold water wake created by the opposite storm.

6. Summary

The motion and evolution of binary tropical cyclones was investigated using a coupled tropical cyclone - ocean movable nested grid model. The model comprises eight-layer atmospheric and seven-layer ocean primitive equation models. In a set of numerical experiments, pairs of axisymmetric weak vortices of both equal and unequal intensity and size were initially separated by specified distances.

The environmental atmospheric and oceanic conditions were set to allow the vortices to rapidly reach hurricane intensities. In most experiments the initial vortices began developing when the influence of their interaction was negligible, and the binary interaction affected their further evolution when the storms reached mature stage.

The experiments showed the existence of a characteristic separation distance that separates the storm attraction from repulsion. This distance is similar to the mutual approach separation (MAS) defined by *Wang and Holland* [1995], and the critical separation distance between barotropic vortices discussed by FKG. In the uncoupled experiments with an SST of 28°C, this separation distance was about 1000 km.

Several regimes of binary storm interaction have been identified, depending on the initial separation distance and the differences in storm strengths. At separation distances of 640 km the interacting storms experienced partial merger (PM). At intermediate (700 km to about 1000 km) initial separation distances, two regimes of storm interaction have been found: straining out (SO) characterized by complete disintegration of the weaker storm and mutual straining out (MSO) characterized by weakening and dissipation of both storms. SO occurred when the interacting storms had substantially different intensities and strengths. MSO was observed when the interacting storms were comparable in size and intensity. In the latter case the storms were unable to approach each other at distances smaller than a certain minimum distance (of about 450-500 km) without being

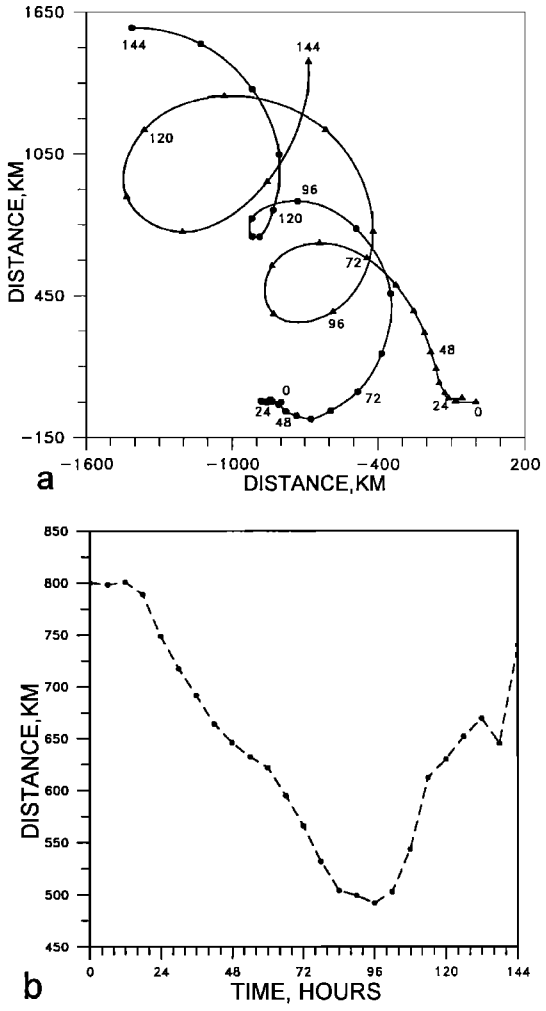

Figure 17. (a) The storm tracks in AOV-800E; numbers denote time in hours; (b) time dependence of separation distance between the storm centers.

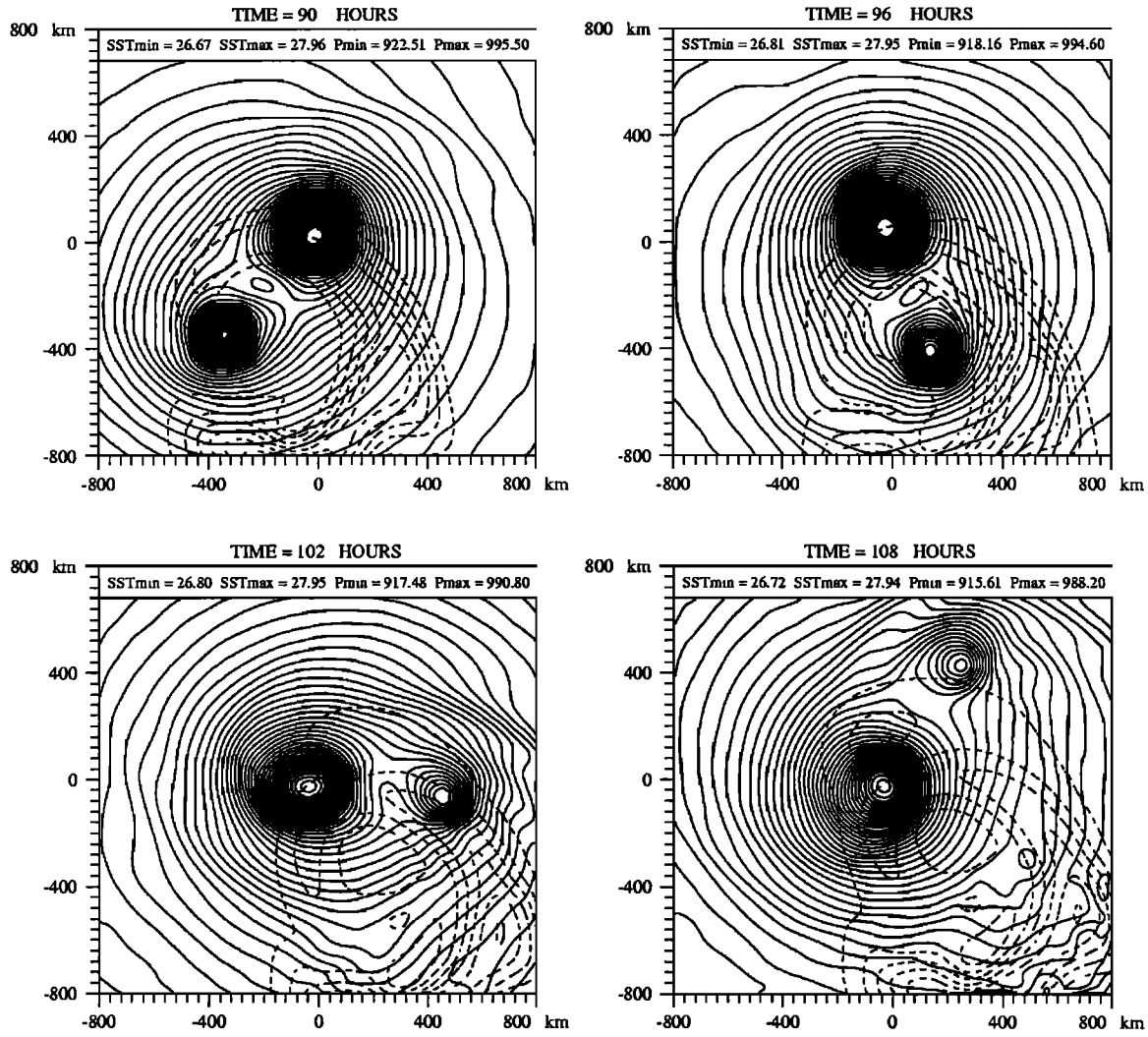

Figure 18. The sea surface pressure (solid lines) and sea surface temperature anomalies (dashed lines) in AOV-800E at different times. The pressure increment is 2 mbar, and the SST increment is 0.2 °C.

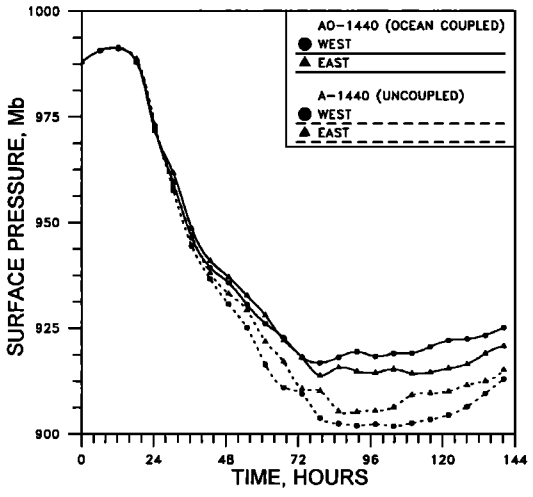

Figure 19. Time series of the minimum sea surface pressure of the storms in A-1440 and AO-1440.

mutually stretched out. Moreover, initial attraction of the storms in this regime was replaced by repulsion, in agreement with observations [*Lander and Holland*, 1993]. One of the possible causes hindering further storm attraction is the displacement of the maximum latent heat release to the opposite sides of the interacting storms. The storms can be pushed away from each other due to the tendency of tropical cyclones to displace toward the areas of maximum heating.

The type of interaction depends on the comparable strength of the storms in a pair. The storm strength, in its turn, depends on various factors such as the Coriolis force, SSTs, and vertical and horizontal shears of the background flow. We found that the result of storm interaction also depends on the initial location of the storms. In our experiments the storms develop from vortices initially at the latitude of 15°N. The storm initially located to the west (storm W) has an advantage over the storm initially located to the east (storm E): The latter storm moves faster northward and turns out to be weaker under other conditions being equal. Thus the result of storm interaction is dependent on what storm (eastern or western) was stronger initially. Note that comparably small changes in structure and strength of interacting storms can

lead to different scenarios of their interaction. This result implies that forecasting the result of binary storm interaction is rather difficult.

The results of a series of sensitivity experiments with different convective parameterization illustrated the importance of adequate simulation of the storm structure for predicting the results of storm interaction. In the experiments conducted with a CISK parameterization of convective heating in a way similar to that used by *Wang and Holland* [1995], the storms were nearly axisymmetric and very compact and continued approaching each other until they merged. Thus the type of storm interaction depends dramatically on the way convective heating is described. This clearly indicates the importance of utilization of realistic convective parameterization.

The ocean coupling may significantly affect the binary storm interaction. The storm-induced SST decrease results in a reduction of storm intensity, slower mutual orbiting and, therefore, substantially different tracks of binary storms. The changes in storm structures due to ocean coupling also cause the decrease of the MAS. The ocean coupling may also change the interaction regime. One of the storms, moving over the cold wake created by the other, can significantly weaken and get destroyed by the stronger counterpart. Thus the ocean coupling may be crucially important in determining which of the storms will be the winner during the storm merger or straining out.

In the study we used terminology of *Dritschel and Waugh* [1992] for just identification of some regimes of storm interaction. For instance, it seemed to us convenient to refer storm coalescence to as "merger", following *Dritschel and Waugh* [1992]. However, *Dritschel and Waugh* [1992] investigated interactions of Rankin-type barotropic vortices and used the results for interpretation of interaction of small-scale turbulent vortices in a turbulent flow. The interaction between barotropic vortices crucially differs from that between baroclinic 3-D tropical cyclones. Here are a few examples of such differences:

(1) *Dritschel and Waugh* [1992] found that merger of barotropic vortices occurred only between equal vortices. In the case of tropical cyclones, merger can take place between storms of significantly different intensities due to radial advection of the weaker storm into the circulation of the stronger one.

(2) Interaction of barotropic vortices has no regimes of mutual straining out and escape occurring after some period of mutual attraction. Interaction between tropical cyclones does include these regimes, which turns out to be of significant importance.

(3) Characteristic scales separating different regimes for barotropic vortices and binary storms are very different, because of the effects of radial advection and the tendency of tropical cyclones to keep and restore their structure.

(4) While the Coriolis force plays no role in the case of interaction of turbulent vortices, its role is very significant in the case of tropical cyclones.

We should note that even in those cases when the interaction between tropical cyclones resembles that of small-scale turbulent vortices, the results are of interest, because the existence of such a similarity is not so obvious.

The regimes of binary storm interaction must also depend on the structure of the background flow. Analyses of the environmental effects will be the subject of our future investigation.

Acknowledgments. This research was supported by the United States-Israel Binational Science Foundation under grant 9500350. I.Ginis was also supported by the U.S. Office of Naval Research under grant 535361.

References

Bender, M. A, I. Ginis, and Y. Kurihara, Numerical simulations of hurricane-ocean interaction with a high resolution coupled model,. *J. Geophys. Res.*, *98*, 23,245-23,263, 1993.

Black, P., and L. K. Shay, Observed sea surface temperature variability in tropical cyclones: Implications for structure and intensity change, paper presented at 21st Conference on Hurricanes and Tropical Meteorology, Miami, Fla., Apr. 24-28, Am. Meteorol. Soc., 1995.

Brand, S., Interaction of binary tropical cyclones of the western North Pacific Ocean, *J. Appl. Meteorol.*, *9*, 433-441, 1970.

Chan, L.C.L., and A. C. K. Law, The interaction of binary vortices in a barotropic model. *Meteorol. Atmos. Phys.*, *56*, 135-155, 1995.

Chang, S. W., A numerical study of the interactions between two tropical cyclones. *Mon. Weather Rev.*, *111*, 1806-1817, 1983.

Chang, S. W., Reply. *Mon. Weather Rev.*, *112*, 1646-1647, 1984.

Deardorff, J. W., Parameterization of the planetary boundary layer for use in general circulation models, *Mon. Weather Rev.*, *100*, 93-106, 1972.

Deardorff, J. W., A multi-limit mixed layer entrainment formulation, *J. Phys. Oceanogr.*, *13*, 988-1002, 1983.

DeMaria, M., and J. C. L. Chan, Comments on "A numerical study of the interactions between two tropical cyclones", *Mon Weather Rev.*, *112*, 1643-1645, 1984.

Dong, K., and C. J. Neumann, On the relative motion of the binary tropical cyclones, *Mon. Weather Rev.*, *111*, 945-953, 1983.

Dritschel, D.G., and D.W. Waugh, Quantification of the inelastic interaction of unequal vortices in two-dimensional vortex dynamics. *Phys. Fluids A*, *4*, 1737-1744, 1992.

Falkovich, A. I., A.P. Khain, and I. Ginis, Evolution and motion of binary tropical cyclones as revealed by experiments with a coupled atmosphere-ocean movable nested grid model, *Mon. Weather Rev.*, *123*, 1345-1363, 1995a.

Falkovich, A. I., A. P. Khain, and I. Ginis, The influence of the air-ocean interaction on the development and motion of a tropical cyclone: Numerical experiments with a triply nested model, *Meteorol. and Atmos. Phys.*, *55*, 167-184, 1995b.

Ginis, I., Ocean response to tropical cyclones, in *Global Perspectives on Tropical Cyclones*, edited by R.Elsberry, chapter 5, pp. 198-260, World Meteorol. Organiz., Geneva, Switzerland, 1995.

Ginis, I., and G. Sutyrin, Hurricane-generated depth-averaged currents and sea-surface elevation,. *J. Phys. Oceanogr.*, *25*, 1218-1242, 1995.

Ginis, I., M. A. Bender, and Y. Kurihara, A numerical study of the tropical cyclone-ocean interaction, in *Tropical Cyclone Disasters*, edited by J. Lighthill, Z. Zhemin, G.J. Holland, and K. Emanuel, pp. 343-355, Peking Univ. Press, Beijing, 1993.

Gray, W., Hurricanes: Their formation, structure and likely role in the tropical circulation, *Meteorology Over Tropical Oceans*, pp.155-218, R.. Meteorol. Soc., Bracknell, England., 1978.

Ivanov, V. N., and A. P. Khain, On parameters determining the frequency of tropical cyclone genesis. *Atmos. and Oceanic Phys.*, *19*, 787-795, 1983.

Jordan, C.L., Mean soundings for the West Indies area, *J. Meteorol.*, *15*, 91-97, 1958.

Khain, A. P., The 12-level axisymmetric numerical tropical cyclone model, *Sov. Meteorol. and Hydrol.*, no.10, 23 – 37, 1979.

Khain, A.P., Modeling of tropical cyclone development on various latitudes, *Sov. Meteorol. and Hydrol.*, no.3, 37-41, 1984.

Khain, A. P., and I. D. Ginis, The mutual response of a moving tropical cyclone and the ocean, *Beitr. Phys. Atmos.*, *64*(2), 125-142, 1991.

Kogan, Y.L., and A. Shapiro, The simulation of a convective cloud in a 3D model with explicit microphysics, II, Dynamical and microphysical aspects of cloud merger, *J. Atmos. Sci.*, *53*, 2525-2545, 1996.

Kurihara, Y., and G. J. Tripoli, Design of a movable nested-mesh primitive equation model, *Mon. Weather Rev.*, *107*, 239-249, 1979.

Kurihara, Y., and R. E. Tuleya, and M. A. Bender, Structure of a tropical cyclone developed in a three-dimensional model, *J. Atmos. Sci. 31*, 893-919, 1974.

Lander, M., and G. J. Holland, On the interaction of tropical-cyclone-scale vortices, I, Observations, *Q. J. R. Meteorol. Soc.*, *119*, 1347-1361, 1993.

Levitus, S., Climotological Atlas of the World Ocean, *NOAA Prof. Pap.*, *13*, 173 pp., U.S. Gov. Print. Off., Washington, D.C., 1982.

Neumann, C. J., Trends in forecasting the tracks of Atlantic tropical cyclones, *Bull. Am. Meterol. Soc.*, *62*, 1473-1485, 1981.

Pokhil, A. E., On formation and destruction of secondary vortices during the interaction of two tropical cyclones (a numerical experiment), *Sov. Meteorol. and Hydrol.*, no.9, 34-41, 1991.

Pokhil, A. E., I. G. Sitnikov, V. A. Zlenko, and I. V. Polyakova, A numerical study of interacting atmospheric vortices, *Sov. Meteorol. and Hydrol.*, no.4, 21-28, 1990.

Ramage, C. S., Interaction between tropical cyclones and the China Sea, *Weather*, *27*, 484-494, 1972.

Ritchie, E. A. and G. J. Holland, On the interaction of tropical-cyclone-scale vortices. II: Discrete vortex patches. *Q. J. R. Meteorol. Soc.*,119, 1363-1379, 1993.

Rosenthal, S. L., Numerical simulation of tropical cyclone development with latent heat by the resolvable scales, I, Model description and preliminary results, *J. Atmos. Sci.*, *35*, 258-271, 1978.

Wang, Y., and G. J. Holland, On the interaction of tropical-cyclone-scale vortices, IV, Baroclinic vortices. *Q. J. R. Meteorol. Soc. 121*, 95-126, 1995.

Willoughby, H. E., and M. B. Chelmow, Objective determination of hurricane tracks from aircraft observations, *Mon. Weather Rev.*, *110*, 1298-1305, 1982.

A. Falkovich, National Center for Environmental Prediction, Environmental Modeling Center, World Weather Building, 5200 Auth Road, Room 7241, Washington, D.C. 20203.

M. Frumin and A. Khain, Institute of the Earth Sciences, Department of Atmospheric Sciences, The Hebrew University of Jerusalem, Givat Ram, Jerusalem, 91904, Israel. (khain@vms.huji.ac.il)

I. Ginis, Graduate School of Oceanography, University of Rhode Island, Narrangasett, RI 02882.

(Received September 14, 1999; revised April 4, 2000;
accepted April 13, 2000.)